UC Berkeley
UC Berkeley Previously Published Works

Title

Energy conservation involving 2 respiratory circuits

Permalink

https://escholarship.org/uc/item/4h81k64t

Journal

Proceedings of the National Academy of Sciences of the United States of America, 117(2)

ISSN

Authors

Schoelmerich, Marie Charlotte
Katsyv, Alexander
Dönig, Judith
et al.

Publication Date

DOI

Peer reviewed

Energy conservation involving 2 respiratory circuits

Marie Charlotte Schoelmerich[a,1] (ID), Alexander Katsyv[a], Judith Dönig[a], Timothy J. Hackmann[b], and Volker Müller[a,2] (ID)

[a]Molecular Microbiology and Bioenergetics, Institute of Molecular Biosciences, Johann Wolfgang Goethe University Frankfurt/Main, 60438 Frankfurt, Germany; and [b]Department of Animal Science, University of California, Davis, CA 95616

Chemiosmosis and substrate-level phosphorylation are the 2 mechanisms employed to form the biological energy currency adenosine triphosphate (ATP). During chemiosmosis, a transmembrane electrochemical ion gradient is harnessed by a rotary ATP synthase to phosphorylate adenosine diphosphate to ATP. In microorganisms, this ion gradient is usually composed of H^+, but it can also be composed of Na^+. Here, we show that the strictly anaerobic rumen bacterium *Pseudobutyrivibrio ruminis* possesses 2 ATP synthases and 2 distinct respiratory enzymes, the ferredoxin:NAD^+ oxidoreductase (Rnf complex) and the energy-converting hydrogenase (Ech complex). In silico analyses revealed that 1 ATP synthase is H^+-dependent and the other Na^+-dependent, which was validated by biochemical analyses. Rnf and Ech activity was also biochemically identified and investigated in membranes of *P. ruminis*. Furthermore, the physiology of the rumen bacterium and the role of the energy-conserving systems was investigated in dependence of 2 different catabolic pathways (the Embden–Meyerhof–Parnas or the pentose–phosphate pathway) and in dependence of Na^+ availability. Growth of *P. ruminis* was greatly stimulated by Na^+, and a combination of physiological, biochemical, and transcriptional analyses revealed the role of the energy conserving systems in *P. ruminis* under different metabolic scenarios. These data demonstrate the use of a 2-component ion circuit for H^+ bioenergetics and a 2nd 2-component ion circuit for Na^+ bioenergetics in a strictly anaerobic rumen bacterium. In silico analyses infer that these 2 circuits are prevalent in a number of other strictly anaerobic microorganisms.

energy conservation | Rnf complex | energy converting hydrogenase | ATP synthase

Chemiosmosis and substrate-level phoshorylation (SLP) are responsible for the formation of the energy currency of any cell, adenosine triphosphate (ATP). During chemiosmosis, a transmembrane electrochemical ion gradient is established by an electron-transport chain (ETC), in which exergonic electron flow is coupled to vectorial ion transport out of the cell. The chemiosmotic gradient is harnessed by highly conserved rotary machines, the ATP synthases (1). These ATP-forming F_1F_O ATP synthases in bacteria or A_1A_O ATP synthases in archaea can either be fueled by an electrochemical H^+ or Na^+-gradient across the cytoplasmic membrane ($\widetilde{\mu}_{H+}$ or $\widetilde{\mu}_{Na+}$). During aerobic respiration, the ETC (respiratory chain) couples NADH oxidation to O_2 reduction, producing water. The electrons are shuttled via membrane-integral complexes (complexes I, III, and IV) and electron carriers (cytochrome and quinones), as well as soluble complexes (complex II and electron transfer flavoprotein [Etf]). This is a highly exergonic process with a Gibbs free-energy change under standard conditions (ΔG_0') of -287 kJ, leading to the establishment of a proton-motive force at complexes I, III, and IV.

Anaerobic microorganisms also use the chemiosmotic mechanism for ATP formation, and some even solely depend on it for energy conservation (2). The electrons derived from catabolite breakdown are channeled via a membrane-integral ETC onto alternative electron acceptors, such as nitrate, sulfate, Fe^{3+}, fumarate, sulfur, and CO_2. Energy-conserving mechanisms in strictly anaerobic bacteria have been thoroughly studied in

acetogenic bacteria. Acetogens use the reductive acetyl-coenzyme A (acetyl-CoA) pathway to fix CO_2 using inorganic gases such as H_2 or CO (autotrophic) or organic compounds such as sugars (heterotrophic) as an electron source. Under autotrophic conditions, they rely on a chemiosmotic mechanism to conserve energy in the form of ATP. Ferredoxin (Fd) is the central electron carrier in bioenergetics of acetogens and fuels 2 distinct respiratory enzymes, the Fd^{2-}:NAD^+ oxidoreductase (Rnf complex) and the Fd^{2-}:H^+ oxidoreductase (Ech complex) (2–4). The Rnf complex in *Acetobacterium woodii* establishes a Na^+ gradient, which fuels a Na^+-dependent ATP synthase. The Ech complex of *Thermoanaerobacter kivui*, on the other hand, leads to the establishment of a H^+ and Na^+ gradient, but it is only the former that is harnessed for energy conservation by the H^+-dependent ATP synthase. In particular, acetogens have been classified as either Rnf- or Ech-containing (5). So far, there are no acetogens that were shown to have Ech and Rnf activity in one cell. Bioinformatic evidence suggested that a number of rumen butyrivibrios astonishingly possess both gene clusters encoding the Rnf and the Ech complex (6, 7). This led us to investigate whether these organisms indeed produce and use both coupling sites, using *Pseudobutyrivibrio ruminis* as model organism.

The butyrivibrios, such as *P. ruminis*, are among the most abundant players in the microbiome of ruminants (8, 9). Their physiological role is to convert sugars to short-chain fatty acids, which are either resorbed by the animal or further metabolized by other microorganisms. They are also responsible for the conversion of "healthy" unsaturated fatty acids from the feedstock to "unhealthy" saturated fatty acids. Therefore, there is a great interest in biomedical research targeting the elucidation of

Significance

The chemiosmotic mechanism is a central mode of energy conservation for microorganisms. It relies on a respiratory chain that couples electron flow at the membrane to the transport of ions across the cytoplasmic membrane. This electrochemical potential fuels a rotary machine, the ATP synthase, to make intracellular ATP. Here, we show that a strictly anaerobic rumen bacterium uses 2 different ion circuits for energy conservation. This is achieved by employing 2 ATP synthases that are driven by a H^+ or Na^+ gradient. The mixed gradient is established by 2 distinct ion pumps. The H^+ gradient is formed by the Ech complex, and the Na^+ gradient is formed by the Rnf complex.

butyrivibrios to decrease the amount of unhealthy fatty acids in dairy and meat (10). The substrate spectrum of the model organism *P. ruminis* is restricted to several C_6 and C_5 sugars (11). This requires the presence of 2 distinct metabolic modules: the Embden–Meyerhof–Parnas pathway (EMPP) for degradation of C_6 compounds and the pentose–phosphate pathway (PPP) for degradation of C_5 compounds. The scope of this work was to analyze whether the Rnf and Ech complexes indeed form active enzymes and to elucidate their physiological role in *P. ruminis*.

Genetic Blueprint of 2 Respiratory Systems in *P. ruminis*

The decryption of rumen butyrivibrio genome sequences led to the identification of several species within these genera that contain both *rnf* and *ech* clusters (6). In the model organism *P. ruminis*, the *ech* cluster is composed of 6 subunits (Fig. 1*A*) that share high sequence similarity with the core Ech complex found in the methanogens *Methanosarcina barkeri* or *Methanosarcina mazei*, but also the Ech complex of *Caldanaerobacter subterraneus* subspecies (subspec.) *tengcongensis* (12). According to the amino acid sequence of the large hydrogenase subunit (EchE), it is classified as a group 4 [NiFe] hydrogenase subgroup 4e (13, 14), just like in *C. subterraneus* subspec. *tengcongensis*. The cluster is preceded by a gene encoding a putative [FeFe] hydrogenase. This hydrogenase is predicted to be cytoplasmic (13) and the only other putative hydrogenase found in the genome. Downstream of the cluster are *hyp* genes that encode the [NiFe] hydrogenase maturation machinery (15).

The *rnf* cluster comprises 6 genes (*rnfCDGEAB*) that are very similar to the *rnf* operon in *A. woodii* (16) (Fig. 1*B*). The putative Rnf complex could be Na^+-dependent as in *A. woodii* or H^+-dependent as in *Clostridium ljungdahlii* (17).

Further inspection revealed that *P. ruminis* also harbors 2 *atpase* clusters (*atpase1* and *atpase2*). Inspection of the genes encoding these 2 F_1F_O ATP synthases showed that they share high sequence similarities, but there are 2 apparent differences. Firstly, the gene encoding the δ subunit of the F_1F_O ATP synthase is missing in the *atpase2* cluster (Fig. 1*D*). This subunit is responsible for linking the α subunit of the F_1 complex with the peripheral stalk, and its role could be compensated by the larger α subunit of the ATPase2. Secondly, the *c* subunit harbors a typical Na^+ binding motif in the *atpase1*, whereas the *atpase2* does not. Thus, one F_1F_O ATP synthase could exploit the $\widetilde{\mu}_{H+}$ (ATPase2) and the other the $\widetilde{\mu}_{Na+}$ (ATPase1) (Fig. 1 *G* and *H*).

Growth and Product Formation of *P. ruminis* Is Stimulated by Na^+

To gain insights into the bioenergetics of the organism, first investigations targeted the growth behavior of *P. ruminis* in the presence or absence of Na^+. When cultivated on 50 mM D-glucose in the presence of Na^+, *P. ruminis* grew with a doubling time of 2.2 h and reached a final OD_{600} of 3.3 after 24 h (Fig. 2). When Na^+ was omitted from the medium (residual Na^+ concentration was 1 mM, and NaCl was substituted with equal amounts of KCl to provide the same ionic strength), cells only started to grow after a significant lag phase of 20 h (Fig. 2). The subsequent doubling time decreased almost 5-fold to 10.3 h, and the final OD_{600} decreased 2-fold to 1.6. The same trend was observed for cultivations on 50 mM D-xylose: The doubling time decreased 4-fold (4.1 and 17.0 h), and the final OD_{600} decreased more than 2-fold (2.6 to 1.1) in the absence of Na^+ (Fig. 2). The high stimulatory effect of Na^+ on growth thus indicates that Na^+ could serve as a coupling ion in *P. ruminis*, but the organism is not strictly dependent on Na^+ for growth.

Both glucose and xylose were always completely consumed under all growth conditions, and the metabolic products were lactate, butyrate, acetate, formate, and molecular H_2. When *P. ruminis* grew on glucose with Na^+, 99% of the carbon was recovered (*SI Appendix*, Table S2) in the form of 59 mM lactate (59%), 19 mM butyrate (25%), 15 mM acetate (10%), and 16 mM formate (5%) (*SI Appendix*, Table S1). The cultures also produced 15 mmol/L medium molecular H_2. In the absence of Na^+, cells only produced about half as much butyrate (10 mM) and also less formate (13 mM), but 3-fold the amount of molecular H_2 (49 mmol/L medium), leading to a decreased carbon recovery of 88%. A very similar trend was observed for cells grown on xylose. A total of 89 or 79% carbon was recovered as lactate (50 or 49%), butyrate (23 or 16%), acetate (11 or 10%), and formate (5 or 4%) in cultivations with or without Na^+ (*SI Appendix*, Fig. S1 and Table S1). Again, H_2 production increased more than 2-fold from 20 to 44 mmol/L medium in the absence of Na^+. The metabolite profiling clearly revealed that less carbon was recovered in the form of the metabolites and that electrons were discarded as molecular hydrogen when cells grew in the absence of Na^+.

Expression Levels of Energy Conserving Systems in *P. ruminis*

To shed some light on the involvement of the 4 energy-conserving complexes under different physiological conditions,
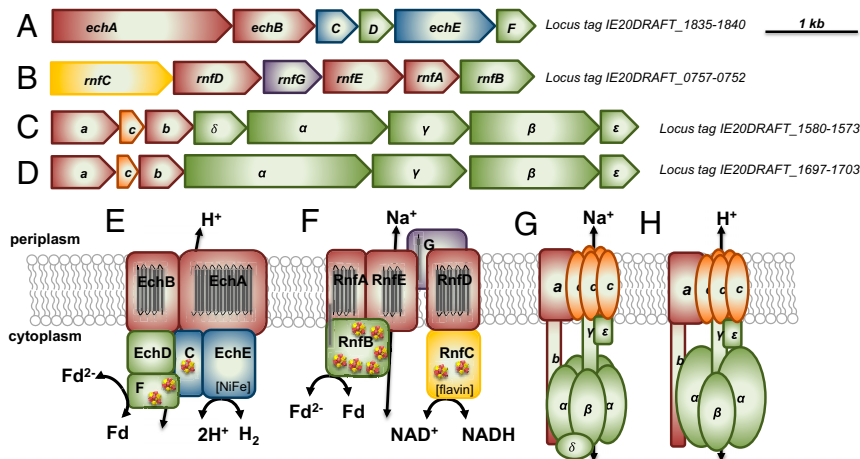
Fig. 1. Genetic arrangement (*A–D*) and hypothetical models (*E–H*) for complexes involved in energy conservation in *P. ruminis*. Dark red, membrane-integral; green, cytoplasmic; blue, hydrogenase; yellow, nicotinamide binding module; purple, periplasmic; orange, coupling ion binding subunits.
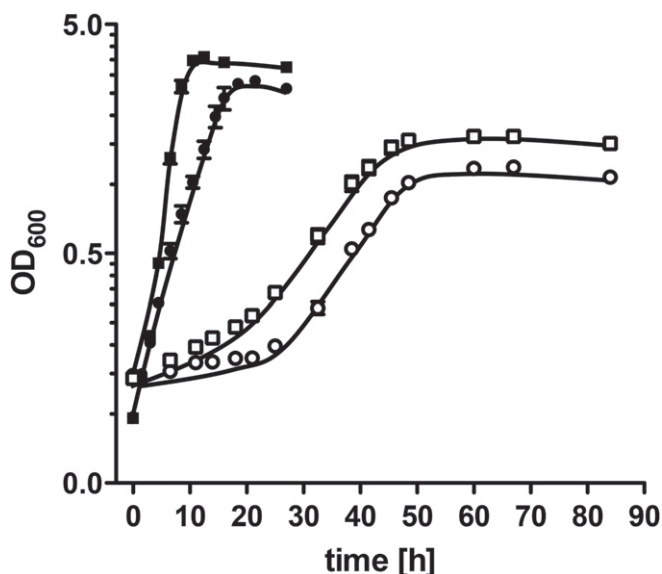
Fig. 2. Growth of *P. ruminis* in the dependence of Na⁺. Cells were cultivated in complex medium containing 97 mM Na^+ (filled symbol) or 1 mM Na^+ (open symbol) in the presence of 50 mM D-glucose (square) or D-xylose (circle).

we analyzed the transcript levels of the *rnf*, *ech*, and *atpase* gene clusters.

First, we assessed the relative expression of the clusters during growth on glucose in dependence of the growth phase. Generally, the expression of all clusters was highest in the early or midexponential growth phase (*SI Appendix*, Table S3). In the late stationary phase, only the *ech* cluster was still highly expressed. The *rnf* cluster was at least 2-fold more highly expressed than the *ech* cluster, and the *atpase* clusters were similarly expressed. A similar trend was observed in cells grown on xylose, with the exception that the *atpase2* cluster showed an up to 20-fold higher expression than the *atpase1* cluster (*SI Appendix*, Table S3). The *atpase2* expression was surprisingly also very high in the early stationary phase, but lower in the midexponential phase. It may be that the H⁺-dependent ATP synthase is important for other cellular processes (e.g., pH homeostasis) that are more important when cells adjust to a new growth phase when they grow on xylose, but not glucose. Either way, based on transcript level, Rnf seems to be more dominant than Ech until cells reach the late stationary phase. Moreover, ATPase2 might play a superior

role during xylose metabolism, probably for purposes other than energy conservation.

Next, we assessed the relative expression of the clusters in the dependence of Na⁺. Interestingly, when cells were grown on glucose without Na⁺, the *ech* and the *atpase2* clusters were highly up-regulated (by a factor of 7.9 and 5.3), and the *atpase1* cluster was up-regulated 2.0-fold, whereas the *rnf* cluster was slightly down-regulated (by a factor of 1.7) compared to the relative transcript level of cells grown with Na⁺ (*SI Appendix*, Fig. S2 and Table S3). A similar trend was observed for the relative expression of *ech* and *rnf* when cells were grown on xylose without Na⁺: *ech* was also up-regulated (1.8-fold), *rnf* was down-regulated (5.1-fold), and *atpase2* was up-regulated (1.7-fold), but *atpase1* was slightly down-regulated (1.3-fold) compared to the expression in cells grown with Na⁺. The data clearly show that *ech* was up-regulated in the absence of Na⁺, and *rnf* was down-regulated at the same time, fostering the notion that Ech could act as a H⁺ pump that takes over the role of the probably Na⁺-dependent Rnf complex. Furthermore, the data suggest that the H⁺-dependent F_1F_O ATP synthase 2 may compensate the role of the Na⁺-dependent F_1F_O ATP synthase 1 in the absence of Na⁺.

Rnf Activity in *P. ruminis*

To elucidate the biochemistry of the energy-conserving complexes, we prepared crude extracts of *P. ruminis* grown until the exponential growth phase on either glucose or xylose, with or without Na⁺. The crude extract was further separated into a membrane and a cytoplasmic fraction via ultracentrifugation. To provide the physiological electron donor of the Rnf, reduced Fd, we purified Fd from *Clostridium pasteurianum* and acetyl-CoA synthase/carbon monoxide dehydrogenase (Acs/CODH) from *A. woodii*, as described previously (4, 18). Subsequently, washed membranes of *P. ruminis* were incubated in assay buffer supplemented with Fd (30 μM) and Acs/CODH (30 μg) under a carbon monoxide (CO) atmosphere at 37 °C. CO was continuously oxidized by the Acs/CODH to provide reduced Fd in a regeneration system. Upon addition of NAD^+ (4 mM), NADH formation was observed as an increase in absorbance at 340 nm (*SI Appendix*, Fig. S3).

The specific Rnf activity of membranes prepared from cells grown on glucose or xylose in the presence of Na⁺ was in the range of 110 to 160 mU/mg, depending on the preparation (Fig. 3A). Negative controls, where 1 component was omitted, did not show NADH formation. The activity was optimal at pH 7.5 with 136 mU/mg and 9, 80, 83, or 29 mU/mg at pH 5.5, 6.5, 8.5, or 9.5.
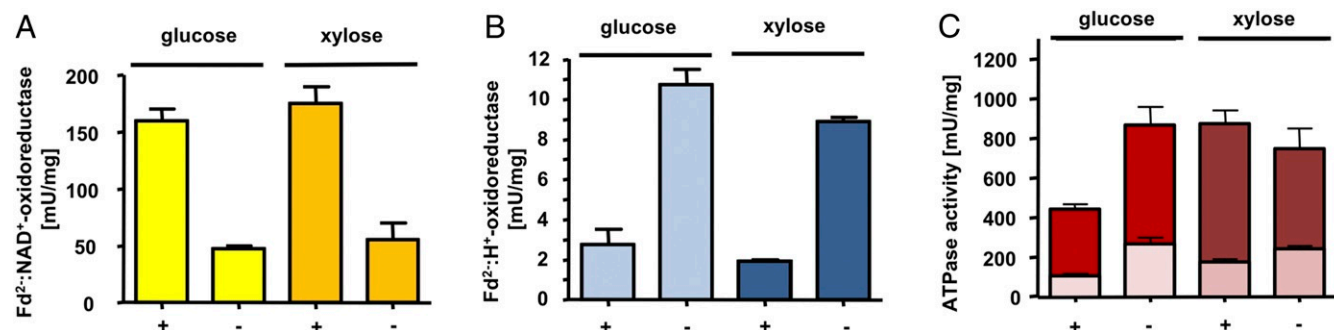
Fig. 3. Rnf, Ech, and ATPase activity in membranes of *P. ruminis*. Rnf (*A*), Ech (*B*), and ATPase (*C*) activity was measured in membranes prepared from cells grown on glucose or xylose with (+) or without (−) Na⁺ at 37 °C. (*A*) Rnf activity was measured in buffer containing 50 mM Tris·HCl, 10 mM NaCl, 4 mM dithioerythritol (DTE), and 4 μM resazurin at pH 7.5 and supplemented with 30 μM Fd, 30 μM Acs/CODH, 340 μg membranes, and 4 mM NAD^+. (*B*) Ech activity was measured in buffer containing 50 mM Mes, 10 mM NaCl, 4 mM DTE, and 4 μM resazurin at pH 6.0 and supplemented with 30 μM Fd. (*C*) ATP hydrolysis was measured in buffer containing 100 mM Tris·HCl, 100 mM maleic acid, and 5 mM MgCl₂ at pH 7.5 with (red) or without (pink) 5 mM Na⁺ (the initial Na⁺ concentration in the Na⁺-free buffer was 68 μM).

To consolidate the notion that the Rnf complex is Na^+-dependent, we analyzed the activity in membranes prepared from cells grown on glucose or xylose with or without Na^+. Indeed, Rnf activity was only 28 or 30% in cells grown without Na^+, with specific activities of 44.14 ± 4.19 or 51.68 ± 24.53 mU/mg, as opposed to 159.83 ± 20.58 or 175.05 ± 21.40 in cells grown with Na^+ on glucose and xylose, respectively ($n = 4$; $\pm$SD) (Fig. 3A). Furthermore, the activity in membranes of glucose-pregrown cells (with Na^+) was 1.5-fold stimulated by 20 mM NaCl in the assay. The observation that *rnf* expression and Rnf activity was higher in cells grown with Na^+ than without, as well as the observed slight stimulation of Rnf activity by Na^+, are strong indications that the Rnf complex is part of the Na^+ circuit.

Ech Activity in *P. ruminis*

Next, we assessed hydrogenase activity in cell-free extracts of *P. ruminis*. Just like the Rnf complex, Ech is typically fueled by Fd^{2-} (2, 19, 20). However, the Fd^{2-} regeneration system proved unsuitable to assess Ech activity, since CO is a potent inhibitor of hydrogenases (*SI Appendix*, Table S4). Hydrogenase activity was not detected by using either nicotinamide NADH or NADPH (4 mM) as reductant (at neither pH 6.0 nor 7.5) (*SI Appendix*, Table S4). The reverse reaction of Ech was measurable by using the artificial dye methylviologen (MV) as the electron acceptor and molecular hydrogen as the electron donor. This H_2-dependent:MV oxidoreductase activity was detected with specific activities of 243 or 52 mU/mg at pH 7.5 or 6.0. However, since the physiological direction should be H_2 evolution rather than oxidation, we searched for alternative assays. An alternative enzyme that provides Fd^{2-} is the pyruvate:Fd oxidoreductase (PFOR). We identified this enzyme activity in crude extracts of *P. ruminis*. The assay contained crude extract (100 to 350 μg), CoA (200 μM), and Fd (60 μM), and formation of Fd^{2-} was detected at 430 nm upon addition of pyruvate (10 mM). The specific activity was 200 to 300 mU/mg. The resulting PFOR-fueled H_2 evolution activity in crude extracts was 1.5 to 4.0 mU/mg, depending on the preparation (*SI Appendix*, Table S4). The activity could be increased by a factor of 1.6, 2.4, or 1.9 when doubling the amount of Fd (120 μM), CoA (400 μM), or pyruvate (20 mM), respectively. The highest activities and easiest assay conditions to measure Ech, however, were to use sodium dithionite (10 mM NaDt) as reductant (*SI Appendix*, Fig. S4). This activity was stimulated by Fd with activities of 3.25 ± 0.92 or 10.65 ± 2.05 mU/mg without or with Fd ($n = 2$; $\pm$SD). Thus, the characteristic reaction of the Ech complex, Fd^{2-}-dependent H_2 formation, was detected in crude extracts and membranes of *P. ruminis*, and NaDt:Fd:H^+ oxidoreductase activity was used to determine Ech activity for subsequent analyses.

To assess the localization of the hydrogenase, the membranes were washed, and hydrogenase activity was monitored in the membranes and supernatant. The crude extract exhibited a total activity (U_{tot}) of 936 mU, and membranes and cytoplasm contained 888 and 254 mU. Washing the membranes once or twice resulted in a decrease in the U_{tot} with 167 or 75 mU and 198 or 101 mU in the respective supernatant fractions. That activity remained in the membranes even after 2 washing steps suggests that membrane-bound Ech was indeed present and active. The loss of activity is likely a result of the dissociation of the hydrophilic hydrogenase module from the hydrophobic Ech core, as described for other multisubunit respiratory enzymes (4, 21–23). Ech is the only membrane-bound hydrogenase encoded by *P. ruminis*. A 2nd hydrogenase is encoded, but it is cytoplasmic (see above). Retention of hydrogenase activity in the membranes thus indicates activity of Ech.

Finally, we assessed Ech activity in washed membranes of *P. ruminis* prepared from cells cultivated on glucose or xylose

with or without Na^+. Indeed, Ech activity was 362 or 468% higher in cells cultivated without Na^+, with specific activities of 11.30 ± 0.95 or 9.00 ± 0.39 mU/mg, as opposed to 3.13 ± 1.22 or 1.93 ± 0.22 in cells grown with Na^+ on glucose and xylose, respectively ($n = 4$; $\pm$SD) (Fig. 3B). The activity (either NaDt:Fd:H^+ or H_2:MV oxidoreductase activity) in membranes of glucose-pregrown cells (with Na^+) could not be stimulated by 20 mM NaCl in the assay. The observation that *ech* expression and Ech activity was higher in cells grown without Na^+ and that Na^+ did not affect the activity are strong indications that the Ech complex is part of the H^+ circuit.

ATPase Activity Is Stimulated by Na^+

To assess the ATP synthases biochemically, we prepared membranes of *P. ruminis* grown on glucose or xylose with or without Na^+ and measured ATP hydrolysis activity.

In Na^+-free buffer (68 μM Na^+), the ATPase activity was 253 or 139% higher in cells grown without Na^+, with specific activities of 265.23 ± 100.81 or 242.65 ± 38.92 mU/mg as opposed to 104.57 ± 25.27 or 173.75 ± 39.99 in cells grown with Na^+ on glucose and xylose, respectively ($n = 4$; $\pm$SD) (Fig. 3C). The higher ATPase activity in cells grown under Na^+-deprived conditions can be explained by a higher abundance of the H^+-dependent ATP synthase 2, which was corroborated by the higher expression of *atpase2* under the same conditions. In Na^+-containing buffer (20 mM NaCl), ATPase activity was generally 3- to 5-fold higher in all membrane preparations than in Na^+-free buffer. This can be explained by the presence of the Na^+-dependent ATPase1, which becomes active once its coupling ion is available. The activity was still 197% higher in membranes prepared from glucose-grown cells without Na^+, with specific activities of 867.43 ± 284.30, as opposed to 440.00 ± 62.44 in cells grown with Na^+ ($n = 4$; $\pm$SD) (Fig. 3C). However, membranes prepared from xylose-pregrown cells without Na^+ possessed a lower specific activity (86%) with 745.45 ± 293.37 mU/mg as opposed to 870.73 ± 194.25 mU/mg in cells grown with Na^+ ($n = 4$; $\pm$SD). This last observation may be explained by the slight up-regulation of the *atpase1* gene in cells grown on xylose with Na^+ (while there was a slight down-regulation in cells grown on glucose with Na^+). The data revealed that there was ATPase activity in Na^+-free buffer, which most likely reflects the H^+-dependent ATPase2. This activity was higher in cells grown without Na^+, matching the expression data for *atpase2*. Moreover, the stimulation of ATPase activity by NaCl demonstrated the presence of the Na^+-dependent ATPase1, and the activity values matched the expression patterns for *atpase1*.

To dissect the Na^+-dependence of the ATPase1 further, we measured the activity in the presence of different concentrations of Na^+, K^+ and Li^+ (Fig. 4A). The determined K_M value for Na^+ was 543 μM. Lithium chloride could partially substitute the stimulatory effect of NaCl, whereas KCl showed no stimulatory effect on ATP hydrolysis activity. Furthermore, the stimulatory effect of NaCl on ATP hydrolysis was investigated at different pH values. At the physiological pH value 7.5, the ATPase activity was stimulated up to 6-fold in the presence of NaCl with a specific activity of 209 mU/mg without Na^+ and 1,303 mU/mg with 2.5 mM added NaCl (Fig. 4B). The same stimulatory effect was observed at pH 6.5 with specific activities of 203 and 1,200 mU/mg without or with 2.5 mM added NaCl (the actual Na^+ concentration of the buffer was 203 μM). The stimulation by NaCl was, however, abolished at pH 5.5 (the actual Na^+ concentration of the buffer was 260 μM). This indicates an inactivation of the Na^+-dependent ATP synthase in the absence of Na^+, leaving only residual activity due to the H^+-dependent ATP synthase.
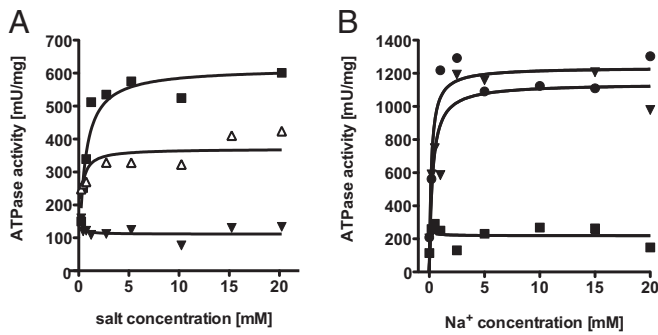
Fig. 4. Stimulation of ATP hydrolysis activity by monovalent salts and by Na⁺ at different pH values. ATP hydrolysis was measured in buffer containing (*A*) 100 mM Tris·HCl, 10 mM maleic acid, and 5 mM $MgCl_2$ at pH 7.5 or (*B*) 50 mM Mes, 50 mM Mops, 50 mM Tris·HCl, 100 mM maleic acid, and 5 mM $MgCl_2$ at pH 5.5 (■), 6.5 (●), or 7.5 (▼) and supplemented with 70 μg of membranes. The reaction was started by adding 3 mM ATP·DiTris, and ATP-dependent formation of inorganic phosphate was measured. (*A*) NaCl (■), LiCl (△), or KCl (▼) was added as indicated. The initial Na⁺ concentration in the buffers was determined to be 243 μM (*A*) or 260 (pH 5.5), 203 (pH 6.5), or 165 μM (pH 7.5) (*B*).

Occurrence of Ech, Rnf, and ATPases in Microbial Genomes

After demonstrating that there is a H⁺ circuit composed of Ech and ATPase2 and a Na⁺ circuit composed of Rnf and ATPase1 in *P. ruminis*, we determined how common these 2 circuits may be in other organisms. We searched the genomes of ~2,900 bacteria and archaea for genes for Ech, Rnf, and ATPases. These genomes are type strains in *Bergey's Manual* (24) that also had a genome sequence that could be readily analyzed [on IMG/M; (25)].

We found that 13 organisms encoded all components of these circuits (Fig. 5 and Dataset S1). These all belong to the phylum Firmicutes and the class Clostridia. Two were *Pseudobutyrivibrio* (*P. ruminis* and *Pseudobutyrivibrio xylanivorans*). Most of the remainder were of the genus *Clostridium* (n = 8).

More organisms encoded "incomplete" circuits. For example, 70 organisms encoded H⁺- and Na⁺-dependent ATPases, but not Ech or Rnf. It is possible that these circuits are truly incomplete. However, it is also possible that they are complete and that ion pumps other than Ech and Rnf complete them. Unmasking the remaining components is a goal for further study.

Discussion

This work demonstrates the existence of 2 bioenergetic circuits in a strictly anaerobic bacterium: a Na⁺ circuit involving Rnf in conjunction with a Na⁺-dependent ATP synthase and a H⁺ circuit involving Ech together with a 2nd H⁺-dependent ATP synthase. This poses a sophisticated strategy in the model rumen bacterium *P. ruminis* to adapt its redox, ion, and energy metabolism.

The rumen is home to about 200 bacterial species that can be cultured (26), with many more that are uncultured (27). *P. ruminis* is part of the "core bacterial microbiome," and its community structure is greatly influenced by the diet of its host (8, 28). In the intestinal tract and the rumen, it has been shown that butyrate and other short-chain organic acids have an inhibitory effect on inflammation (29, 30). This symbiosis between host and microbe may be better when Na⁺ is abundant, since we demonstrated an increase in microbial fitness and thus production of butyrate in the model rumen bacterium *P. ruminis*.

P. ruminis generates most of its ATP from substrate-level phosphorylation in the EMPP or PPP and from butyrate production (Fig. 6 and *SI Appendix*, Fig. S7). The chemiosmotic gradient is only a 2nd mode of energy conservation, but nev-

ertheless essential for all sorts of cellular processes, including transport, motility, and ion and pH homeostasis. The experiments presented herein demonstrate that *P. ruminis* uses both a Na⁺ and a H⁺ circuit for chemiosmosis.

When cells grow on glucose or xylose, these sugars are converted to pyruvate via the EMPP or PPP at the gain of ATP and reducing equivalents in the form of NADH (Fig. 6 and *SI Appendix*, Fig. S7). Pyruvate is metabolized further to lactate by the lactate dehydrogenase at the cost of NADH, and this was in fact the main product measured under all growth conditions. Pyruvate is also converted to acetyl-CoA via PFOR (at the gain of Fd^{2-}) or via the pyruvate formate lyase. Since PFOR activity was measured in crude extracts and formate was quantified in the supernatants, both enzymes are present and active in the organism. The acetyl-CoA is then further converted via acetyl-phosphate to acetate by the phosphotransacetylase and the acetate kinase, gaining ATP. The acetyl-CoA is finally used for butyrate production in several steps at the cost of NADH and gain of Fd^{2-} and ATP. Therefore, the catabolic route leads to the formation of ATP from SLP and reducing equivalents in the form of NADH and Fd^{2-}. These reducing equivalents must then be reoxidized to allow a continuation of the catabolism, and this is where the ion circuits come into play.

Under Na⁺-rich conditions, electrons are shuttled into both circuits to regenerate NADH by the Rnf complex or discard excess electrons in the form of H_2 by the Ech complex (Fig. 6*A*). Concomitantly, a Na⁺ and a H⁺ gradient is established by the Rnf and Ech complex, which is harnessed by the ATPase1 and ATPase2 for energy conservation. The high NADH pools lead to more butyrate production. Since butyrate formation involves the electron-bifurcating butyryl–CoA/Etf complex (Bcd/Etf) (31), Fd^{2-} is generated from the simultaneous reduction of crotonyl–CoA and Fd with NADH (Fig. 6; enzymes 4 and 6). This refuels the Rnf complex at the gain of more ATP and regain of NADH,
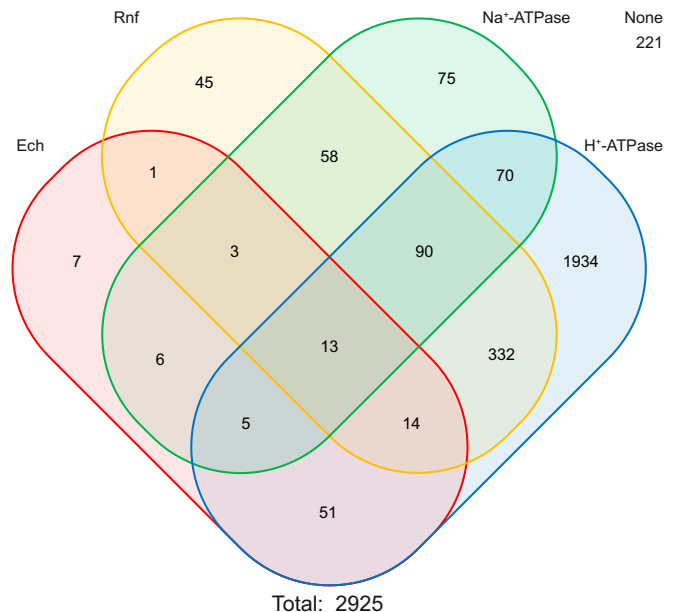
Fig. 5. Several organisms may have 2 bioenergetic circuits. Genomes of n = 2,925 bacteria and archaea were searched for genes encoding Ech, Rnf, and ATP synthases. The Venn diagram shows the number of organisms encoding each combination of these enzymes. Enzymes were encoded if genes for all subunits were found. The ATPases were distinguished into Na⁺- and H⁺-dependent types based on the amino acid sequence of subunit *c*. See Dataset S1 for a full list of genomes and locus tags for genes.
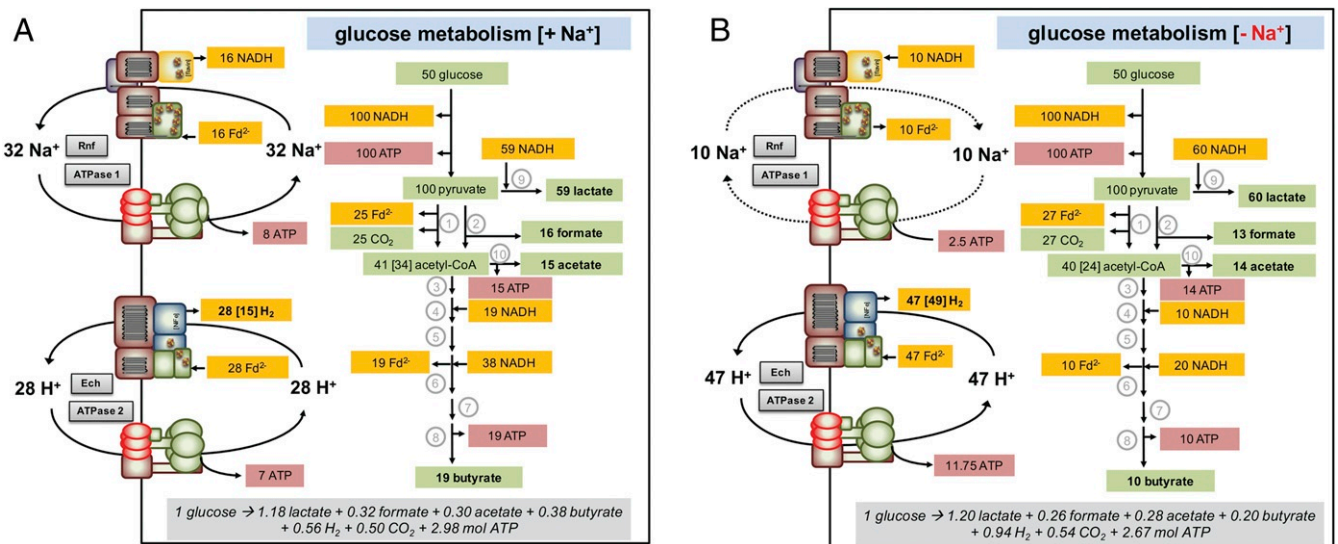
Fig. 6. Redox-balanced models for glucose metabolism in *P. ruminis* involving 2 chemiosmotic circuits. Models for metabolism in cells grown with (*A*) or without (*B*) Na$^+$ are shown. The numbers indicate the moles of substance degraded or produced, as determined in this study (bold) or calculated. In brackets are the actual measured H$_2$ amounts or the acetyl-CoA moieties recovered as organic acids detected, whereas the numbers outside the brackets result from calculations. The ATP synthase has an assumed rotor stoichiometry of 12/3, and Rnf and Ech are assumed to translocate 1 or 0.5 ions per electron transferred, respectively. Green, carbon compounds; yellow, reducing equivalents; red, energy in the form of ATP. 1, PFOR; 2, pyruvate formate lyase; 3, thiolase; 4, 3-hydroxybutyryl–CoA dehydrogenase; 5, crotonase; 6, Bcd–Etf complex; 7, CoA-transferase; 8, kinase; 9, lactate dehydrogenase; 10, acetate kinase.

leading to better cellular fitness (reflected in the stimulation of growth by Na$^+$).

Under Na$^+$-deprived conditions, there is an excess of reducing equivalents in the form of NADH when cells are grown on glucose (Fig. 6*B*). The lack of Na$^+$ severely slows down the Na$^+$ circuit and thus the interconversion of NADH and Fd pools. The H$^+$ circuit must now maintain the membrane potential and immediate redox homeostasis. The NAD$^+$ required for a continuation of catabolism may be regenerated by the Na$^+$ circuit running in reverse: A Na$^+$-pumping ATPase1 fuels the regeneration of NAD$^+$ from NADH oxidation and Fd reduction at the Rnf complex. This hypothesis is supported by the fact that Na$^+$ could not be completely abolished in the Na$^+$-free medium, and such a Na$^+$-gradient-consuming role for the Rnf complex is described in other metabolisms, such as lactate metabolism in *A. woodii*, for example (32). In cells grown on xylose without Na$^+$, the redox-balanced models indicate that the Na$^+$ circuit is not required, because redox balancing is achieved by the Ech complex and the electron flow during product formation (*SI Appendix*, Fig. S7). Under both metabolisms (glucose and xylose), the calculated ATP yields are lower in the absence of Na$^+$, which is a consequence of the ATP-depleting Na$^+$ circuit (glucose) or shutdown of the Na$^+$ circuit (xylose), as well as decreased butyrate production. The latter entails less available redox energy (in the form of Fd^{2-}) to fuel energy conservation via the circuits. Ultimately, the lower theoretical ATP yields in combination with very slow redox maintenance is most likely the reason for the severely decreased fitness of *P. ruminis* grown in the absence of Na$^+$.

Putting this into perspective of the physiological conditions, feeding large amounts of grain can reduce the pH in the rumen to well below 5.5 (33), which could lead to an inactivation of ATPase1 (Fig. 4*B*) and concomitantly a shutdown of the Na$^+$ circuit. However, normally the Na$^+$ concentration in the rumen is at least 60 mM and can be up to 500 to 800 mM (34). Therefore, both circuits are finetuned to ensure microbial fitness of *P. ruminis* and ultimately of the host, by providing health-promoting organic acids. Moreover, higher ATP pools may contribute to biohydrogenation of unsaturated fatty acids

(35) via a membrane-associated oxidoreductase (36). This process is tied to the provision of reducing equivalents, but neither to ATP formation nor changed when H$^+$ are replaced by an unsaturated fatty acid as electron acceptor (6).

Besides the "core microbiome," the rumen is also home to methanogenic archaea and acetogenic bacteria (37–39), and both Rnf and Ech have been identified and characterized in these groups of strict anaerobes (2, 3, 40). The H$_2$ evolved from Ech can be scavenged by these members. Furthermore, they could be responsible for the emergence of both *rnf* and *ech* clusters in several rumen butyrivibrios (6) via horizontal gene transfer (41). After all, it is the ecological environment comprising a diverse consortium that made the occurrence of Ech and Rnf possible and advantageous for *P. ruminis*.

It is likely that rumen butyrivibrios are not the only groups of organisms that use both Ech and Rnf for separate chemiosmotic circuits. Intriguingly, acetogens were postulated to rely either on Rnf or Ech (5), but the decryption of more genomes revealed a cooccurrence of *rnf* and *ech* genes in some (14). It will be particularly interesting to investigate in these organisms, which depend on the chemiosmotic gradient for energy conservation (acetogens and methanogens), whether they also use 2 circuits for energy conservation.

Material and Methods

Experimental procedures for cultivation of the organism; cell harvest and preparation of crude extracts and membranes; measurement of Ech, Rnf, and ATP hydrolysis activity; determination of relative transcript levels; determination of metabolites, pH, and Na$^+$ concentrations; and the search for Ech, Rnf, and ATases in microbial genomes are described in *SI Appendix, SI Materials and Methods*.

Data Availability Statement. Data discussed in the paper are available in Datasets S1–S3.

1. F. Mayer, V. Müller, Adaptations of anaerobic archaea to life under extreme energy limitation. *FEMS Microbiol. Rev.* **38**, 449–472 (2014).

2. M. C. Schoelmerich, V. Müller, Energy conservation by a hydrogenase-dependent chemiosmotic mechanism in an ancient metabolic pathway. *Proc. Natl. Acad. Sci. U.S.A.* **116**, 6329–6334 (2019).

3. E. Biegel, V. Müller, Bacterial Na^+-translocating ferredoxin:NAD^+ oxidoreductase. *Proc. Natl. Acad. Sci. U.S.A.* **107**, 18138–18142 (2010).

4. V. Hess, K. Schuchmann, V. Müller, The ferredoxin: NAD^+ oxidoreductase (Rnf) from the acetogen *Acetobacterium woodii* requires Na^+ and is reversibly coupled to the membrane potential. *J. Biol. Chem.* **288**, 31496–31502 (2013).

5. K. Schuchmann, V. Müller, Autotrophy at the thermodynamic limit of life: A model for energy conservation in acetogenic bacteria. *Nat. Rev. Microbiol.* **12**, 809–821 (2014).

6. T. J. Hackmann, J. L. Firkins, Electron transport phosphorylation in rumen butyrivibrios: Unprecedented ATP yield for glucose fermentation to butyrate. *Front. Microbiol.* **6**, 1–11 (2015).

7. T. J. Hackmann, D. K. Ngugi, J. L. Firkins, J. Tao, Genomes of rumen bacteria encode atypical pathways for fermenting hexoses to short-chain fatty acids. *Environ. Microbiol.* **19**, 4670–4683 (2017).

8. G. Henderson *et al.*, Rumen microbial community composition varies with diet and host, but a core microbiome is found across a wide geographical range. *Sci. Rep.* **5**, 14567 (2015).

9. D. R. Caldwell, M. P. Bryant, Medium without rumen fluid for nonselective enumeration and isolation of rumen bacteria. *Appl. Microbiol.* **14**, 794–801 (1966).

10. M. R. Maia *et al.*, Toxicity of unsaturated fatty acids to the biohydrogenating ruminal bacterium, *Butyrivibrio fibrisolvens*. *BMC Microbiol.* **10**, 52 (2010).

11. N. O. van Gylswyk, H. Hippe, F. A. Rainey, *Pseudobutyrivibrio ruminis* gen. nov., sp. nov., a butyrate-producing bacterium from the rumen that closely resembles *Butyrivibrio fibrisolvens* in phenotype. *Int. J. Syst. Evol. Microbiol.* **46**, 559–563 (1996).

12. R. Hedderich, L. Forzi, Energy-converting [NiFe] hydrogenases: More than just H_2 activation. *J. Mol. Microbiol. Biotechnol.* **10**, 92–104 (2005).

13. D. Sondergaard, C. N. Pedersen, C. Greening, HydDB: A web tool for hydrogenase classification and analysis. *Sci. Rep.* **6**, 34212 (2016).

14. M. C. Schoelmerich, V. Müller, Energy-converting hydrogenases: The link between H_2 metabolism and energy conservation. *Cell. Mol. Life Sci.*, 10.1007/s00018-019-03329-5 (2019).

15. P. M. Vignais, B. Billoud, Occurrence, classification, and biological function of hydrogenases: An overview. *Chem. Rev.* **107**, 4206–4272 (2007).

16. E. Biegel, S. Schmidt, J. M. González, V. Müller, Biochemistry, evolution and physiological function of the Rnf complex, a novel ion-motive electron transport complex in prokaryotes. *Cell. Mol. Life Sci.* **68**, 613–634 (2011).

17. P. L. Tremblay, T. Zhang, S. A. Dar, C. Leang, D. R. Lovley, The Rnf complex of *Clostridium ljungdahlii* is a proton-translocating ferredoxin:NAD^+ oxidoreductase essential for autotrophic growth. *mBio* **4**, e00406–12 (2012).

18. P. Schönheit, C. Wäscher, R. K. Thauer, A rapid procedure for the purification of ferredoxin from Clostridia using polyethylenimine. *FEBS Lett.* **89**, 219–222 (1978).

19. B. Soboh, D. Linder, R. Hedderich, A multisubunit membrane-bound [NiFe] hydrogenase and an NADH-dependent Fe-only hydrogenase in the fermenting bacterium *Thermoanaerobacter tengcongensis*. *Microbiology* **150**, 2451–2463 (2004).

20. C. Welte, U. Deppenmeier, Bioenergetics and anaerobic respiratory chains of aceticlastic methanogens. *Biochim. Biophys. Acta* **1837**, 1130–1147 (2014).

21. J. D. Fox, R. L. Kerby, G. P. Roberts, P. W. Ludden, Characterization of the CO-induced, CO-tolerant hydrogenase from *Rhodospirillum rubrum* and the gene encoding the large subunit of the enzyme. *J. Bacteriol.* **178**, 1515–1524 (1996).

22. A. Tersteegen, R. Hedderich, *Methanobacterium thermoautotrophicum* encodes two multisubunit membrane-bound [NiFe] hydrogenases. transcription of the operons and sequence analysis of the deduced proteins. *Eur. J. Biochem.* **264**, 930–943 (1999).

23. V. Hess *et al.*, Occurrence of ferredoxin:NAD^+ oxidoreductase activity and its ion specificity in several Gram-positive and Gram-negative bacteria. *PeerJ* **4**, e1515 (2016).

24. W. B. Whitman, *Bergey's Manual of Systematics of Archaea and Bacteria* (Wiley, New York, 2015).

25. I. A. Chen *et al.*, IMG/M v.5.0: An integrated data management and comparative analysis system for microbial genomes and microbiomes. *Nucleic Acids Res.* **47**, D666–D677 (2019).

26. R. Seshadri *et al.*, Cultivation and sequencing of rumen microbiome members from the Hungate1000 collection. *Nat. Biotechnol.* **36**, 359–367 (2018).

27. M. Kim, M. Morrison, Z. Yu, Status of the phylogenetic diversity census of ruminal microbiomes. *FEMS Microbiol. Ecol.* **76**, 49–63 (2011).

28. C. L. Elliott *et al.*, Using 'omic approaches to compare temporal bacterial colonization of *Lolium perenne*, *Lotus corniculatus*, and *Trifolium pratense* in the rumen. *Front. Microbiol.* **9**, 2184 (2018).

29. K. E. Bach Knudsen *et al.*, Impact of diet-modulated butyrate production on intestinal barrier function and inflammation. *Nutrients* **10**, 1499 (2018).

30. H. Dai *et al.*, Sodium butyrate ameliorates high-concentrate diet-induced inflammation in the rumen epithelium of dairy goats. *J. Agric. Food Chem.* **65**, 596–604 (2017).

31. F. Li *et al.*, Coupled ferredoxin and crotonyl coenzyme A (CoA) reduction with NADH catalyzed by the butyryl-CoA dehydrogenase/Etf complex from *Clostridium kluyveri*. *J. Bacteriol.* **190**, 843–850 (2008).

32. M. C. Weghoff, J. Bertsch, V. Müller, A novel mode of lactate metabolism in strictly anaerobic bacteria. *Environ. Microbiol.* **17**, 670–677 (2015).

33. T. G. Nagaraja, E. C. Titgemeyer, Ruminal acidosis in beef cattle: The current microbiological and nutritional outlook. *J. Dairy Sci.* **90**, E17–E38 (2007).

34. F. R. Bell, The relative importance of the sodium ion in homeostatic mechanisms in ruminant animals. *Proc. R. Soc. Med.* **65**, 631–634 (1972).

35. D. Paillard *et al.*, Relation between phylogenetic position, lipid metabolism and butyrate production by different *Butyrivibrio*-like bacteria from the rumen. *Antonie Van Leeuwenhoek* **91**, 417–422 (2007).

36. P. E. Hughes, W. J. Hunter, S. B. Tove, Biohydrogenation of unsaturated fatty acids. Purification and properties of *cis*-9,*trans*-11-octadecadienoate reductase. *J. Biol. Chem.* **257**, 3643–3649 (1982).

37. P. H. Janssen, M. Kirs, Structure of the archaeal community of the rumen. *Appl. Environ. Microbiol.* **74**, 3619–3625 (2008).

38. B. R. Genthner, C. L. Davis, M. P. Bryant, Features of rumen and sewage sludge strains of *Eubacterium limosum*, a methanol- and H_2-CO_2-utilizing species. *Appl. Environ. Microbiol.* **42**, 12–19 (1981).

39. F. Rieu-Lesme, B. Morvan, M. D. Collins, G. Fonty, A. Willems, A new H_2/CO_2-using acetogenic bacterium from the rumen: Description of *Ruminococcus schinkii* sp. nov. *FEMS Microbiol. Lett.* **140**, 281–286 (1996).

40. C. Welte, C. Krätzer, U. Deppenmeier, Involvement of Ech hydrogenase in energy conservation of *Methanosarcina mazei*. *FEBS J.* **277**, 3396–3403 (2010).

41. A. Calteau, M. Gouy, G. Perriere, Horizontal transfer of two operons coding for hydrogenases between bacteria and archaea. *J. Mol. Evol.* **60**, 557–565 (2005).

MICROBIOLOGY